Nonlinear Dynamics (2005) 41: 111–128

Nonlinear System Analysis with Karhunen–Loève Transform

PHILIPP GLÖSMANN and EDWIN KREUZER*
Mechanik und Meerestechnik, Technische Universität Hamburg-Harburg, 21073 Hamburg, Germany;
**Author for correspondence (e-mail: kreuzer@tu-hamburg.de; fax: +49-40-42878 2028)*

(Received: 3 February 2004; accepted: 7 June 2004)

Abstract. The Karhunen–Loève Transform was established to find structures in random process data. Nonlinear dynamical systems often appear to have uncorrelated output in case of chaotic behavior. This analogy leads to the idea of analyzing nonlinear dynamical systems with methods developed for random processes. The Karhunen–Loève Transform provides a basis for different approaches to the investigation of these systems. This paper gives an introduction to the mathematical concept and an overview of popular Karhunen–Loève Transform applications. It focuses on approaches to state monitoring of nonlinear dynamical systems based on experimental data.

Key words: coherent structures, Karhunen–Loève-Transform, model reduction, nonlinear dynamics, proper orthogonal decomposition, random excitation

1. Introduction

In scientific research or technical development there is a strong demand for model order reduction and data compression. Models shall be as simple as possible, but still display all system properties of interest. The question arising in this context is: What is the minimum number of *state variables/eigenforms* that have to be considered? Of course the answer depends on the goal of the investigation as well as on the type of system itself. While for special problems there may be a trivial solution, very often researchers have to rely on their experience for the choice of *state variables/eigenforms*.

The Karhunen–Loève Transform (KLT), also known as proper orthogonal decomposition or principle component analysis, was initially designed to analyze random process data by introducing new coordinate systems based on the statistical properties of the processes. It does not only provide structures within random data, but also leads to more efficient ways of coordinate description. These characteristics make the KLT a suitable tool for various tasks ranging from data analysis and compression to model order reduction. Depending on the individual application, the KLT helps to find the minimum number of *state variables* and *eigenforms* based on the structure of the system-dynamics.

For the purpose of system analysis, the KLT has been applied to stationary state systems only. We will show that the KLT also helps to investigate nonlinear dynamical systems during states of *non-stationary behavior*. After a brief introduction of the mathematical concept in Section 2, an overview of current Karhunen–Loève Transform applications is given in Section 3. Approaches to state monitoring of nonlinear dynamical systems based on experimental data are discussed in Section 4, where the results of the analysis are also presented.

2. Karhunen–Loève Transform

The KLT is the linear transform, that best approximates a stochastic process in least squares sense [1]. It can be formulated for both continuous- and discrete-time. This paper focuses on the discrete KLT to

process sampled measurement data. The derivation of the continuous KLT is similar and can be found in typical textbooks for signal analysis.

The mathematical theory of the KLT relies upon the properties of Hilbert Spaces. A *Hilbert Space* $\mathcal{H}$ is a vector space in $\mathbb{R}^n$ or $\mathbb{C}^n$, that is complete as a metric space and has a scalar product $\langle \cdot, \cdot \rangle$. The norm is defined as $\|\phi\| = \sqrt{\langle \phi, \phi \rangle}$ for $\phi \in \mathcal{H}$ and the metric is defined as $d(\phi, \psi) = \|\phi - \psi\|$ for $\phi, \psi \in \mathcal{H}$. Without loss of generality we will regard Hilbert Spaces in $\mathbb{R}$ in this paper, only.

The concept of *orthogonality* and *orthonormality* is crucial for the derivation of the KLT: Two vectors $\phi_i, \phi_j \in \mathcal{H}$ are orthogonal if $\langle \phi_i, \phi_j \rangle = 0 \; \forall \, i, j$ with $i \neq j \wedge \langle \phi_i, \phi_j \rangle \neq 0$ for $i = j$. A basis $\mathbf{\Phi}$ of vectors in a Hilbert Space is an orthonormal basis if any two distinct vectors $\phi_i, \phi_j \in \mathbf{\Phi}$ are orthogonal and in addition $\|\phi\| = 1 \, \forall \, \phi \in \mathbf{\Phi}$.

Let $\mathbf{y}$ be a real-valued zero-mean random process, that can be expressed as a vector function

$$\mathbf{y} = \begin{pmatrix} y_1 \\ \vdots \\ y_n \end{pmatrix}, \quad \mathbf{y} \in \mathbb{R}^n, t \in \mathbb{R}. \tag{1}$$

The restriction to zero-mean process does not imply any limitation of generality, since any process $\mathbf{z}$ with mean $\mathbf{m}_z$ can be translated into a zero-mean process $\mathbf{y}$ by

$$\mathbf{y} = \mathbf{z} - \mathbf{m}_z. \tag{2}$$

The choice of a basis for the vector function is arbitrary as long as it spans the correct embedding dimension. With an orthonormal basis $\mathbf{\Psi} = \{\psi_1, \ldots, \psi_n\}$ the process can be written as

$$\mathbf{y} = \mathbf{\Psi} \boldsymbol{\alpha}, \tag{3}$$

where $\boldsymbol{\alpha}$ is the representation

$$\boldsymbol{\alpha} = [\alpha_1, \ldots, \alpha_n]^{\mathrm{T}}. \tag{4}$$

It is given by

$$\boldsymbol{\alpha} = \mathbf{\Psi}^{\mathrm{T}} \mathbf{y}. \tag{5}$$

We derive the KLT by demanding uncorrelated coefficients

$$E\{\alpha_i \alpha_j\} = \lambda_j \delta_{ij}, \quad i, j = 1, \ldots, n, \tag{6}$$

where the scalars λ_j with $j = 1, \ldots, n$ are yet unknown real numbers with $\lambda_j \geq 0$ and Kronecker-symbol δ_{ij}.[1] Substituting Equation (5) into Equation (6) we obtain

$$E\left\{\psi_i^{\mathrm{T}} \mathbf{y} \mathbf{y}^{\mathrm{T}} \psi_j\right\} = \lambda_j \delta_{ij}, \quad i, j = 1, \ldots, n. \tag{7}$$

[1] $\delta_{ij} = \begin{cases} 1 & \text{for } i = j \\ 0 & \text{else} \end{cases}$

We then can factor out both ψ of the expectance value in Equation (7) since they are no random variables, but the unknown basis vectors of the KLT. Treating $\mathbf{y}$ as the realization of a random process, we can formulate

$$\mathbf{R}_{yy} = E\{\mathbf{y}\mathbf{y}^{\mathrm{T}}\} \tag{8}$$

which allows us to write Equation (7) as

$$\boldsymbol{\psi}_i^{\mathrm{T}}\mathbf{R}_{yy}\boldsymbol{\psi}_j = \lambda_j\delta_{ij}, \quad i, j = 1, \ldots, n. \tag{9}$$

It is obvious that because of $\boldsymbol{\psi}_i^{\mathrm{T}}\boldsymbol{\psi}_j = \delta_{ij}$, Equation (9) is satisfied if the vectors $\boldsymbol{\psi}_i$, $i = 1, \ldots, n$, are solutions of the eigenvalue problem

$$\mathbf{R}_{yy}\boldsymbol{\psi}_i = \lambda_i\boldsymbol{\psi}_i, \quad i = 1, \ldots, n. \tag{10}$$

Matrix $\mathbf{R}_{yy}$ is the covariance matrix of process $\mathbf{y}$ and provides the eigenvalue problem with the following properties:

– The covariance matrix is diagonal, which implies that $\mathbf{R}_{yy}$ is *positive (semi-)definite*; that is, only real eigenvalues exist and all $\lambda_i \geq 0$.
– Eigenvectors that belong to different eigenvalues are orthogonal to each other.
– If multiple eigenvalues exist, their eigenvectors are linearly independent and can be chosen orthonormal.

The solution of (10) leads to a basis of n linearly independent eigenvectors that span the 'sample space', this is the space embedded in $\mathbb{R}^n$ that contains all possible realizations of the n-dimensional process $\mathbf{y}$. The orthonormal KLT-basis is obtained by normalization (e.g. by Gram-Schmidt-Procedure). Basis vectors $\boldsymbol{\psi}_i$ are referred to as '*Characteristic Functions*' and representations α_i, with $\lambda_i = E\{\alpha_i\alpha_i\}$, are called '*Weighing Factors*'.

Geometrically, the KLT can be interpreted as a change of coordinate systems to describe any set in $\mathcal{H}$. Figure 1 displays the transformation in $\mathbb{R}^2$: the KLT basis vectors ψ_1 and ψ_2 lie on the principal axes of the sample data, with the new coordinates α_1 and α_2.

Among all properties of the Karhunen–Loève-Transform the following three are the most striking for its application in dimension reduction:

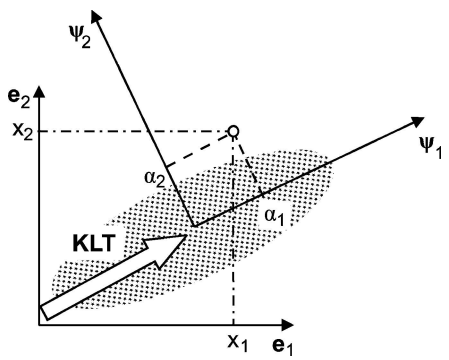

Figure 1. KLT coordinate transform.

1. It can be proven (ref. e.g. to [1]) that among all orthonormal linear transforms the KLT yields the smallest possible error.
2. The *Parseval's Relation*[2] holds. This means that the sum over all α_i^2 equals the signal power of process **y**.
3. According to (3) process **y** can be expressed by the sum over the products of the *Characteristic Functions* and the *Weighing Factors*. Whereas each eigenvalue determines the importance (energy content) of the corresponding *Characteristic Function* to the process signal.

As the different forms of application are discussed, we will refer to these properties and display their contribution to the individual KLT usage.

3. Popular Applications of KLT

Due to the fact that the *Characteristic Functions* of the KLT are not predetermined, but are calculated in dependence on the processed data, the Karhunen–Loève-Transform is extremely adaptive. This makes the KLT a universal tool for various tasks. In this section the following most popular applications of KLT are discussed:

– Signal analysis (Section 3.1),
– Model reduction (Section 3.2),
– Optimal control (Section 3.3),
– Template matching (Section 3.4),
– Compressive image encoding (Section 3.5).

For the investigation of nonlinear dynamical systems, the KLT has been mainly used to reduce the order of applied mathematical models. In Section 4, we introduce a new approach to nonlinear dynamical system analysis via KLT.

We will allow process **y** to characterize any engineering system, even those that cannot be described by differential equation. We will allow **y** to depend on two different variables: Time $t \in \mathbb{R}$ and position $\mathbf{x} \in \mathbb{R}^3$. In order to analyze *multi-dimensional* systems, we will define the n-dimensional process $\mathbf{y}(\mathbf{x}, t)$. Regarding *discrete-time* processes only, the time variable t turns into $k \in \mathbb{N}$; where $t = k\delta t$ with the fixed sampling interval δt. Now the realizations of process **y** at discrete time form a $k \times n$-matrix.

3.1. Signal Analysis

In system analysis, the Discrete-Fourier-Transform (DFT) is a means to decompose a sampled signal into harmonic functions and to determine the frequency coefficients. Let us consider the *one-dimensional* process signal $y(k)$ as a function of discrete time k. Then, this process can be expressed by Fourier-series expansion as

$$y(k) = \frac{1}{N} \sum_{\ell=0}^{N-1} \alpha_\ell W_N^{-\ell k}, \tag{11}$$

where α_ℓ are the *Weighing Factors*, $W_N^{-\ell k}$ are the *Characteristic Functions*. The abbreviation W_N denotes the complex exponential functions

$$W_N = e^{-i\frac{2\pi}{N}}. \tag{12}$$

[2] The inner product of two vectors equals the inner product of their representations with respect to an orthonormal basis.

These depend on the total number N of available data points, that also determines the evaluated discrete frequencies $\omega_\ell = \ell/N$.

The KLT is not only a means for random data analysis, but is also capable of decomposing *deterministic* signals. The process $y(k)$ also may be expressed by Karhunen–Loève series expansion of *Weighing Factors* α_ℓ and *Characteristic Functions* $\psi_\ell(k)$ as

$$y(k) = \sum_{\ell=1}^{N} \alpha_\ell \psi_\ell(k). \tag{13}$$

Let us compare the Discrete Fourier with the Karhunen–Loève-Transform. There are some special properties that both share. The DFT and the KLT are linear transforms, that
– decompose a signal into a set of *Characteristic Functions* together with their *Weighing Factors*,
– operate in bidirectional order,
– have an orthogonal basis, and
– obey the Parseval's Relation [1].

The major difference between the DFT and KLT stems from their sets of bases, the *Characteristic Functions*. While for the DFT this is the predetermined set of harmonic functions, for the KLT the basis depends upon the stochastic properties of the observed process. The KLT just gives the algorithm to derive an individual orthonormal basis for each signal.

The bases of DFT and KLT determine their approximation performance. Due to its basis, the DFT is most efficient for decomposing sine functions, thus possibly leading to ineffective transforms of non-harmonic signals. The KLT algorithm is adaptive, it provides the optimal linear transform (ref. Section 2) of any kind of signal. In the special case of periodic signals, the bases of KLT and DFT are similar, differing only in amplitude.

For KLT signal analysis we have to assume, that process $y(k)$ is short-time stationary for the duration of the longest time-structure, that we wish to observe. Data sets are gathered to form the process' covariance matrix $\mathbf{C}_{yy}$. This is done by the '*method of snapshots*'[3]: we treat signal $y(k)$ as a spatially expanded one-dimensional process and read the entire data set

$$\mathbf{y}(k) = \begin{pmatrix} y_1(k) \\ y_2(k-1) \\ \vdots \\ y_n(k-(n-1)) \end{pmatrix} \in \mathbb{R}^n \tag{14}$$

with finite time-history of $n-1$ data samples at each time k. Then, the time-index k is increased and the next data set $\mathbf{y}(k+1)$ is stored. After n consecutive readings, the covariance matrix is formed. We now can solve (10) for the *Characteristic Functions* and then can project $\mathbf{y}(k)$ onto this basis to derive the *Weighing Factors*.

3.2. Model Reduction

The idea to reduce complexity of system models by KLT was initiated by the investigation of fluid flow dynamics. In 1967, Lumley introduced the concept of extracting dominant structures from turbulent

[3] This method was introduced by Sirovich [2] for fluid flow analysis (see Section 3.2).

flow by proper orthogonal decomposition [3]. This approach is discussed in detail by Dellnitz et al. [4], Holmes et al. [5], Newman [6] and Steindl et al. [7], to name just a few. The general idea is to expand the *Partial Differential Equation* (PDE) in a Galerkin-ansatz:

$$\mathbf{y}(\mathbf{x}, k) = \sum_{\ell=1}^{N} \alpha_\ell(k)\psi_\ell(\mathbf{x}). \tag{15}$$

Let $\mathbf{y}(\mathbf{x}, k)$ be the function of a PDE, describing the spatial expansion of a dynamical system. For separation of *time-dependent* from *space-dependent* differential equations, the series (15) can be interpreted as the projection of $\mathbf{y}(\mathbf{x}, k)$ onto the basis $\mathbf{\Psi}$ of *Characteristic Functions*. Model reduction is achieved, if the expansion (15) is truncated at a fixed number $M < N$; with $M, N \in \mathbb{N}$ (for examples we refer to [8, 9]).

As mentioned in Section 2, the KLT does not only provide an orthonormal basis. For dynamical systems, the *Weighing Factors* display the mean importance of the corresponding *Characteristic Functions* to the KLT-series expansion. In the case of velocity, the square of the *Weighing Factors* can be interpreted as the *kinetic energy* of the individual mode. Due to this characteristic, the KLT is well suited for model dimension reduction: The series expansion (15) is truncated to contain an arbitrarily chosen portion of system energy; this is $E_{\text{kin}} = \sum_\ell^M \alpha_\ell^2$ and only the first corresponding M *Characteristic Functions* are considered. The error (neglected energy) can be calculated by the sum over the remaining weights; where $e(M) = \sum_\ell^{N-M} \alpha_\ell^2$.

Due to the nature of KLT, the basis $\mathbf{\Psi}$ cannot be determined a priori, but can only be derived from existing data. To form the covariance matrix, the spatially expanded, dynamical system $\mathbf{y}(\mathbf{x},k)$ is simulated and data is collected from discrete points $\mathbf{x}$ at times k (*method of snapshots* [2, 6]). Each snapshot is treated as the kth realization of process $\mathbf{y}(\mathbf{x})$.

3.3. Optimal Control

For linear controllers of multi-dimensional systems with a single control variable u, a weighing function $\mathbf{k}_R$ is used in the feedback-branch of the control loop. Stability and performance of the controlled system depend upon the choice of $\mathbf{k}_R$. The KLT provides a straight forward method to derive its components based on the system dynamics. For the dynamical behavior of engineering systems, one wants to keep the kinetic energy at minimum to avoid dispensable wear. Kreuzer, Kust and Struck [10–12] have applied the KLT to drill strings in simulation and small-scale experiment to determine $\mathbf{k}_R$ for optimal control. The equations for a typical controller can be written as

$$\begin{aligned} \dot{\mathbf{y}} &= \mathbf{f}(\mathbf{y}) + \mathbf{b}u, \\ z &= \mathbf{k}_R^{\mathrm{T}}(\mathbf{y}_s - \mathbf{y}), \\ u &= w + k_P \ z + k_I \int z\, dt, \end{aligned} \tag{16}$$

where $\mathbf{y}$ and $\mathbf{y_s} \in \mathbb{R}^n$ are the state vector and reference state, respectively, $\mathbf{b} \in \mathbb{R}^n$ is the mapping vector, $w \in \mathbb{R}$ is the desired movement and k_P and $k_I \in \mathbb{R}$ are the controller's proportional and integral gain factors [13].

If all system states[4] are observable, the weighing function $\mathbf{k}_R$ can be determined by KLT: The state vector is interpreted as the realization of a random process. First data sets of $\mathbf{y}(k)$ are collected.

[4] In case of the drill-string, the number of states is $m = 2 \times n$ (n: system dimension).

Remember, that the KLT provides the optimal least square approximation for mean time, only. Therefore, we have to consider transient states apart from states of stationary motion. We also have to differentiate between displacements and velocities within the state vector $\mathbf{y}$.

Focusing on kinetic energy, we form the covariance matrix solely from the deviations in displacement. The KLT provides a set of *eigenvalues* and *Characteristic Functions*. As discussed in the previous section, these can be interpreted as *eigenforms* of the system dynamics. Eigenvalues λ_ℓ describe the kinetic energy of the *Characteristic Functions* ψ_ℓ. To minimize the kinetic energy, we form the weighing function as

$$\mathbf{k}_R = \begin{pmatrix} \psi_1(1) \\ \vdots \\ \psi_1(n) \\ \mathbf{0} \end{pmatrix}. \tag{17}$$

Of all *Characteristic Functions* the first one covers the greatest portion of kinetic energy. Therefore, we choose ψ_1 for the first n entries in $\mathbf{k}_R$. We do not consider the velocity-variables, therefore the last n entries in (17) are set to zero.

3.4. Template Matching

Coherent structures are not only of interest in the analysis of complex system dynamics. The challenge to find and identify characteristic properties appears in pattern recognition problems, also. Template matching finds a pattern in the obtained data set $\mathbf{y}(\mathbf{x}, k)$ that is similar to a given reference $\hat{\mathbf{y}}(\mathbf{x}, k)$. The variety of KLT-applications ranges from image recognition (see e.g. [14, 15]) via speech analysis (e.g. [16]) to applications in medicine (e.g. [17]).

For template matching we arrange the data in vectorial form, were each data point has a certain position and property $y(x, k)$. We form the '*template*' from a collection of '*training vectors*', where all tolerable deviations from the ideal template have to be covered. These *training vectors* are normalized to zero mean values and unit standard deviation. From the normalized vectors we form the covariance matrix and determine *eigenvalues* together with *Characteristic Functions* ψ_ℓ. The normalized ideal template $\hat{\mathbf{y}}$ then is projected onto the KLT-basis $\hat{\mathbf{\Psi}}$ and its representing *Weighing Factors* $\hat{\boldsymbol{\alpha}}$. The recognition process can be accelerated, if the KLT-series expansion of the ideal template $\hat{\mathbf{y}} = \sum_{\ell=1}^{N} \hat{\alpha_\ell}\hat{\psi}_\ell$ is truncated at $\ell = M (M < N)$ and only the remaining $\hat{\boldsymbol{\alpha}}_M$ and $\hat{\mathbf{\Psi}}_M$ are stored.

We perform template matching of new, normalized data vectors $\tilde{\mathbf{y}}$ by projecting them onto the reduced KLT-basis $\hat{\mathbf{\Psi}}_M$. We can determine the similarity of the new data vector with the template by calculating the deviation $\mathbf{e} = \|\tilde{\boldsymbol{\alpha}} - \hat{\boldsymbol{\alpha}}_M\|$.

3.5. Compressive Image Encoding

In electronic form, pictures consist of pixel-matrices, where each pixel has a position and a color. In principle, the data compression is performed by truncating the KLT-series expansion of the image data (for a detailed description, see e.g. ref. [18]).

The pixel-matrix is divided into a set of adjacent '*range blocks*' of uniform dimension. The content of each range block is mapped into a vector $\mathbf{y}_k$ and is interpreted as one realization of $\mathbf{y}(x, k)$, where position x is a scalar. The realizations are used to form the covariance matrix: The range blocks are normalized

to zero mean and unit standard deviation. From the covariance matrix the *Characteristic Functions* are calculated to form a basis. Each range block is projected onto this basis and its representation (vector of *Weighing Factors*) is truncated at a predetermined length. The resulting image encoding consists basically of the *Characteristic Functions* for the truncated KLT-series expansion and then for each range block of the normalization parameters and the *Weighing Factors*.

The KLT seems to be best suited for data compression, since the color information of each pixel can be regarded as deviation from a mean value. Thus the KLT provides the optimal basis for a truncated series expansion, since a large portion of the color information is covered within the first few *Characteristic Functions*. However, due to its complex derivation, there is a threshold in picture-size beyond which other algorithms, such as Discrete Cosine or Wavelet Transform, lead to more efficient data processing [19].

4. State Analysis

In the previous section we have discussed various applications of KLT. In the case of dynamical processes $\mathbf{y}(k)$ (Sections 3.2 and 3.3) the mathematical models were known and the systems were investigated at stationary states.

In this section we want to introduce an approach to utilize the KLT for state monitoring. A poorly observable nonlinear dynamical system, a rolling railway wheelset, is investigated by means of KLT. We want to characterize the system-state and observe state changes.

4.1. Railway Wheelset Rolling State

Riding comfort and safety of trains predominantly depend upon the dynamics of its wheelsets. The rail-wheel contact is essential for the behavior of the wheelset, since any distortion or defect of the rail surface excites vibration. In literature (e.g. [20, 21]) the condition of wheelset vibration is referred to as its *'rolling state'*. One goal of a joint research project,[5] is to monitor and characterize the wheelset rolling states on an objective basis. At present, there exist expressions *'healthy'* for a smooth railway-ride and *'unhealthy'* for a bumpy one, to describe the wheelset dynamics. This characterization is merely based upon rather subjective criteria such as the noise emitted.

The wheelset dynamics excited by the rail–wheel contact are highly nonlinear. Significant progress has been made in this area during recent years (e.g. ref. [22, 23]), most models of wheel-rail contact are based on the approach introduced by Kalker [24]. However, the problem of determining the correct friction coefficient, that is subject to major changes, due to moisture and lubricants, persists. A model-based analysis seems to be too complicated for the on-line analysis of the wheelset rolling state. For this reason we apply the KLT to measurement data, gathered from railway wheelset experiment in order to monitor the wheelset dynamics.

Naturally, the monitoring of dynamics is limited to the degrees of freedom (DOF) that are observable. A wheelset considered as a rigid body has six DOF. Accounting also for structural vibrations of its axle in first flexural and torsional modes, we would need a minimum of 12 coordinates for completely defining the system: There are six coordinates necessary for description of the rigid-body-motion and additional three coordinates each, for the monitoring of the first torsional and bending modes (e.g. ref. [25]).

[5] Laufzustandsmonitoring von Eisenbahnradsätzen, Bundesministerium für Bildung und Forschung.

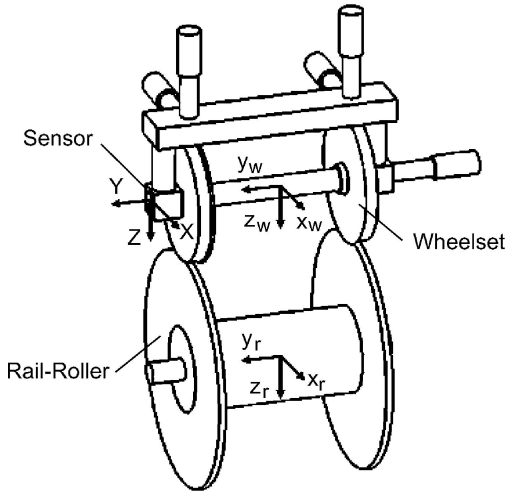

Figure 2. Wheel/rail-roller test-rig.

In order to create a simple test set-up, the sensors have to be placed outside any rotating parts of the railway wheelset. This is part of a trade-off, since in return for this inexpensive mock-up, the observability of the wheelset is limited: a 3D-accelerometer is attached to the wheelset suspension (see Figure 2) measuring the accelerations along the body-fixed wheelset-axis. As a consequence the bending and torsional deflections of the axle are not observable. However, these vibrations will contribute to the acceleration measurements as periodic oscillations, if excited.

4.2. Experimental Test Set-up

Experimental tests were performed at the wheel/rail-roller test-rig of Deutsche Bahn AG.[6] Figure 2 displays the test set-up in principle: a standard wheelset, suspended at the ends of its axle, is driven by a rotating rail-roller. As a kinematic linkage, the wheel-rail contact-curve couples the *roll angle* (rotation about x_w-axis) and the position in y_w-z_w-plane of the wheelset. Hydraulic cylinders act as the spring-mounted car load on the wheelset in z_w-direction and also control its x-/y-position and its *yaw angle* (rotation about z_w-axis). A 3D-acceleration sensor, attached to the left unsprung suspension, measures the wheelset dynamics.

During the tests stationary conditions such as constant rotating speeds, constant applied loads were provided, and the x-position of the wheelset was fixed. All experiments were conducted with a controlled wheelset y-position. The rotating speed of the rail-roller was varied from 50 to 80 km/h for similar test series. We found the results discussed in this section to be typical for the yaw angle changes at the test site and that within the given limits, the speed does not change the wheelset dynamics qualitatively.

Table 1 displays the parameter settings for the experiments analyzed in this section: the wheelset is placed in a *'neutral'* position: The y-axes of the wheelset and the rail-roller are aligned in parallel and the wheelset is situated vertically on top of the rail-roller. The y-position of the wheelset is chosen to eliminate any lateral force, such that the rolling wheelset will keep this position without guidance. An electric motor drives the rail-roller with a constant speed and the upper hydraulic cylinders apply a constant load to the wheelset. For each test series the yaw angle between the wheelset and the rail-roller

[6] DB Systemtechnik, TFZ 95, Brandenburg-Kirchmöser.

Table 1. Parameter set for wheel/rail-roller experiments.

Experiment	Speed (km/h)	Yaw angle (mrad)	Load (tons)
W110	80	0	12
W120	80	1.5	12
W130	80	2.5	12
W140	80	3.5	12
W150	80	2.5	12
W160	80	1.5	12
W170	80	0	12

was increased within three steps from 0 to 3.5 mrad. During the experiment with the largest yaw angle, the test members emitted a well noticeable noise.

4.3. KLT-Approach

The wheelset dynamics are highly nonlinear, that we might regard any set of measurement data at discrete time k as one realization of a multi-dimensional random process. Thus we may apply KLT and treat the sensor signals as random processes. As proposed in Sections 3.2 and 3.3, the measurement data $\mathbf{y}(k)$ is arranged as spacial components of the time-dependent process

$$\mathbf{y}(k) = \begin{pmatrix} y_1(k) \\ \vdots \\ y_n(k) \end{pmatrix}, \quad \mathbf{y} \in \mathbb{R}^n, k \in \mathbb{R}. \tag{18}$$

The measurement vector $\mathbf{y}$ contains the data of all sensor signals.

The KLT-approach to the wheelset rolling state analysis is to use correlations in the measurement data collected from rolling wheelsets. Since the wheelsets are physical devices and obey laws of nature, one expects an order behind the data sets. The KLT emphasizes correlation of the different sensor signals thus helping to find some structure in the measured dynamics.

If there are characteristic wheelset dynamics during certain different *rolling states*, then the KLT will help to display these. But before we apply the KLT in our analysis, some requirements have to be checked.

4.3.1. *Requirements for KLT-Application*

Let us assume that occurrences and qualities of the railway irregularities and surface defects are distributed randomly along the track length. Then the wheelset is subject to random excitation. As long as the train car moves at subcritical speeds[7] and the disturbances are somewhat moderate, the wheelset is an asymptotically stable system. The motion of a single wheelset is well investigated. Its state trajectories are known to lie on attracting limit cycles. Each excitation means a deviation of the current wheelset rolling state from its present trajectory. It follows any trajectory only piecewise up to the next

[7] The dynamical stability of a wheelset depends upon its velocity as one bifurcation parameter. At subcritical speed, the rail-wheelset system is asymptotically stable in sense of Lyapunov. At the critical speed, this systems undergoes a Hopf-bifurcation and becomes unstable (for a detailed discussion refer to [26]).

excitation. Since these occur on a random basis, each new initial trajectory position is the outcome of a random experiment. In between two excitations the wheelset motion can be regarded as '*stationary*'. Depending upon the measure one takes, these distances can become infinitely small. For the wheelset rolling state characterization, we will differentiate between negligible distortions, that we will accredit to the regular wheelset dynamics as major disturbances, that will alter the wheelset rolling state.

The KLT requires a single monitored process to be ergodic (see e.g. [5]) for the derivation of the covariance matrix. We assume the mechanical parts of the wheelset and its suspension to deteriorate gradually. Thus, we can regard the experimental setup to remain unchanged for each realization and the wheelset dynamics to be an ergodic process. Now we can calculate the covariance matrix for each interval of *stationary* wheelset rolling state between two excitations. For practical reason, we predefine a constant time interval $\Delta T = [a, b]$ for which we calculate the covariance matrix. It is obvious that the length of ΔT has a great influence on the matrices and on the KLT outcome as well.

4.3.2. *KLT-Results*

Solving the eigenvalue problem (10), the KLT provides us with one $k \times n$ matrix of *Weighing Factors*, one set of *n eigenvalues* and one basis of *n Characteristic Functions* for each ΔT. Since we assume the wheelset dynamics to be short-time stationary for the duration of ΔT, the wheelset rolling state can be characterized by these three sets of KLT-results:

1. The *Weighing Factors* are the coordinates of the projection of $\mathbf{y}(k)$ onto the KLT-basis. They contain the *time-dependent* information of the transformed wheelset dynamics and can be interpreted as the amplitude of the wheelset dynamics in the direction of the corresponding *Characteristic Function*.
2. The *eigenvalues* are the squares of the *Weighing Factors* (6). Each eigenvalue determines the contribution of the corresponding *Characteristic Function* to the process' $\mathbf{y}(k)$ signal power. We we will thus interpret the eigenvalues as the wheelset's '*surrogate*[8] *kinetic power*' in the direction of the corresponding *Characteristic Function*.
3. The *Characteristic Functions* span the signal space and lie in direction of its principal axes. As in mechanical system analysis, we will interpret them as the eigenforms of the system dynamics. In case of the railway wheelset we get a set of *n* decoupled *Characteristic Functions*, the '*surrogate eigenforms*'.

Stationary motion of nonlinear dynamical systems will lead to fixpoints, limit cycles or tori in state space description. As the wheelset is periodically driven, its trajectories in state space will describe limit cycles or fixpoints. State trajectories derived from the vector of sensor signals $\mathbf{y}(k)$ display the superposition of all eigenforms. The transformed state vector, consisting of the *Weighing Factors* and their integral over time, shows trajectories whose components are decoupled. These decoupled components can be analyzed separately. Similar to the *eigenvalues* the *Weighing Factors* display the amplitude/power of the system motion in the direction of the *Characteristic Functions*. In the case of negligible power content of these (indicated by small *eigenvalues*), the limit cycles degenerate to fixpoints. Additionally, we could investigate the *Weighing Factors* for dominant frequencies, e.g. by Wavelet Transform.

For nonlinear dynamics, especially for mechanical systems, kinetic energy is a major bifurcation parameter. While at low energies, these systems tend to be asymptotically stable, they bifurcate and turn unstable if their kinetic energy increases. Therefore, in a first approach we will analyze the *eigenvalues*, *surrogate power* to differentiate between wheelset rolling states. This approach complies with the idea that a wheelset's kinetic energy is minimum for smooth rolling and increases upon excitation. Due to the

[8]The expression '*surrogate*' is chosen, because instead of displacements or velocities the sensors measure forces and accelerations.

small dimension of $\mathbf{y}(k)$, the Karhunen–Loève dimension,[9] as suggested by [27, 28], is not considered suitable to characterize wheelset rolling states.

To limit the KLT-analysis to the *eigenvalues*, *surrogate power*, fails short. Although the *Characteristic Functions* are constant for each interval of short-time stationary wheelset rolling state, they change according to wheelset dynamics. If different eigenforms are excited within two consecutive time intervals, the *Characteristic Functions* of the sensor signals will respond. Making use of the good approximation properties of KLT, we only need to consider a limited number of *surrogate eigenforms* to describe the wheelset dynamics adequately. Thus we can characterize the wheelset rolling state by the *Characteristic Functions* of the largest one or two *eigenvalues*.

4.3.3. *Sensitivity of KLT-Analysis*

We want to investigate the sensitivity of the proposed KLT-analysis to changes in signal properties from the previous interval $\Delta\hat{T} = [\hat{a}, \hat{b}]$ to the following $\Delta T = [a, b]$. Without limitation on generality, for the following analytical investigation we will consider a two-dimensional signal vector $\mathbf{y}(k)^{\mathrm{T}} = [x(k)\, z(k)]$. Let $x(k)$ and $z(k)$ be the signals of two time-dependent processes that are stationary for $k \in [a, b]$. The auto-covariances are determined by

$$c_{xx}(m) = \frac{1}{N}\sum_{k=1}^{N}(x(k) - x_m)(x(k+m) - x_m) \tag{19}$$

and

$$c_{zz}(m) = \frac{1}{N}\sum_{k=1}^{N}(z(k) - z_m)(z(k+m) - z_m). \tag{20}$$

The cross-covariance can be calculated by

$$c_{xz}(m) = \frac{1}{N}\sum_{k=1}^{N}(x(k) - x_m)(z(k+m) - z_m), \tag{21}$$

with x_m, y_m mean signal values, $m, k \in [a, b]$, $N \in \mathbb{N}$, where $m + N \leq b - a$. For the cause of KLT-analysis we set the shift factor to $m = 0$.

Although wheelset and suspension dynamics are nonlinear, we assume the sensor signals to be coupled in the sense that additional excitation of the system will either lead to an increase in all sensor signal amplitudes or will increase some and will leave all others unchanged. We assume, that additional excitation will not lead to the increase and decrease of different sensor signal amplitudes at the same time. We will also assume, that mean signal values remain unchanged.

Then we may denote the changes of signals $x(k)$, $z(k)$ due to additional excitation by multiplication of the previous signals $\hat{x}(k)$, $\hat{z}(k)$ with scaling factors $\alpha(k)$, $\beta(k)$, resulting in

$$x(k) = \alpha(k) \cdot \hat{x}(k) \tag{22}$$

and

$$z(k) = \beta(k) \cdot \hat{z}(k), \tag{23}$$

[9] The Karhunen–Loève dimension is defined by the number of *Characteristic Functions* from KLT, necessary to capture a given fraction of the total energy or *surrogate kinetic power* in case of the railway wheelset, respectively.

respectively. We allow α and β to vary with k. For $k \in [a, b]$ there will be lower and upper bounds of $\alpha(k)$ and $\beta(k)$. Let us consider an increase in signal amplitude. Then we can find

$$1 \leq \alpha_{\min} \leq \alpha(k) \leq \alpha_{\max} < \infty \tag{24}$$

and

$$1 \leq \beta_{\min} \leq \beta(k) \leq \beta_{\max} < \infty. \tag{25}$$

Applying Equations (22) and (23), the current cross-covariances can be calculated by

$$c_{xz} = \frac{1}{N} \sum_{k=1}^{N} (\alpha(k)\hat{x}(k) - x_m)(\beta(k)\hat{z}(k) - z_m) \tag{26}$$

for which we can find upper and lower limits for c_{xz}, such that $c_{xz\,\min} \leq c_{xz}(k) \leq c_{xz\,\max}$. Solving (26) for the minimal change in cross-covariance and considering only zero mean signals[10] gives

$$\begin{aligned} c_{xz\,\min} &= \alpha_{\min}\beta_{\min} \frac{1}{N} \sum_{k=1}^{N} \hat{x}(k)\hat{z}(k) \\ &= \alpha_{\min}\beta_{\min}\hat{c}_{xz}. \end{aligned} \tag{27}$$

The cross-covariance c_{xz} of signals $x(k)$ and $z(k)$ of the excited system exceeds the cross-covariance $\hat{c}_{xz}$ of the previous time interval by at least the factor $\alpha_{\min} \cdot \beta_{\min}$:

$$\hat{c}_{xz} \leq c_{xz\,\min} = \alpha_{\min}\beta_{\min}\hat{c}_{xz} \leq c_{xz}(k) \leq c_{xz\,\max} = \alpha_{\max}\beta_{\max}\hat{c}_{xz}. \tag{28}$$

Similar approximations can be obtained for the auto-covariances

$$\hat{c}_{xx} \leq c_{xx\,\min} = \alpha_{\min}^2\hat{c}_{xx} \leq c_{xx}(k) \leq c_{xx\,\max} = \alpha_{\max}^2\hat{c}_{xx} \tag{29}$$

and

$$\hat{c}_{zz} \leq c_{zz\,\min} = \beta_{\min}^2\hat{c}_{zz} \leq c_{zz}(k) \leq c_{zz\,\max} = \beta_{\max}^2\hat{c}_{zz}. \tag{30}$$

The covariance matrices become

$$\hat{C}_{xz} = \begin{pmatrix} \hat{c}_{xx} & \hat{c}_{xz} \\ \hat{c}_{xz} & \hat{c}_{zz} \end{pmatrix} \tag{31}$$

for the previous interval and

$$C_{xz\,\min} = \begin{pmatrix} \alpha_{\min}^2\hat{c}_{xx} & \alpha_{\min}\beta_{\min}\hat{c}_{xz} \\ \alpha_{\min}\beta_{\min}\hat{c}_{xz} & \beta_{\min}^2\hat{c}_{zz} \end{pmatrix} \tag{32}$$

[10] This does not impose any limitation on generality, since we can always apply Equation (2). In addition, the sensors utilized for the experimental setup where scaled to zero mean.

for the additional excited system. Solving the eigenvalue problem (10) for $C_{xz\,\min}$, we obtain

$$\lambda_{1,2\,\min} = \frac{1}{2}\left(\alpha_{\min}^2 \hat{c}_{xx} + \beta_{\min}^2 \hat{c}_{zz}\right) \pm \sqrt{(\alpha_{\min}\beta_{\min})^2 A + \frac{1}{4}B}, \tag{33}$$

with $A = (\hat{c}_{xz}^2 - \frac{1}{2}\hat{c}_{xx}\hat{c}_{zz})$ and $B = (\alpha_{\min}^4 \hat{c}_{xx}^2 + \beta_{\min}^4 \hat{c}_{zz}^2)$.

Let $\alpha_{\min} < \beta_{\min}$, then we derive the lower limit for $\lambda_{1,2}$

$$\lambda_{1,2\,\min} > \alpha_{\min}^2 \hat{\lambda}_{1,2}. \tag{34}$$

An upper bound for the maximal *eigenvalue* $\lambda_{1,2\,\max}$ can be derived in the same way for the increase of signal amplitudes. Also, a similar calculation can be performed to find minimal and maximal values for the eigenvalue in case of a decrease in signal amplitudes.

If the amplitudes of the sensor signals rise due to an increased excitation, the KLT-eigenvalues (λ_i) of the current time-interval will differ from those ($\hat{\lambda}_i$) of the previous. An increase in the signal amplitudes α_i leads to an increase in the λ_i. From (34) we can observe, that all current eigenvalues λ_i will at least increase by the square of the minimal signal amplitude rising factor $\alpha_{\min}$. This means for the state observation of the railway wheelset dynamics:

– Minor disturbances, that do not qualitatively change the wheelset rolling state, lead to small increases in signal amplitudes. These will lead to negligible changes in the *eigenvalues*.
– Major additional excitations, that drastically change the wheelset rolling state, lead to larger increases in signal amplitudes. Due to (34) one can detect these qualitative changes by monitoring the *eigenvalues*. Since these will change at least by the square of the smallest rising factor $\alpha_{\min}$, major additional excitations will be accentuated by KLT.

4.4. Analysis Results

For the investigation of the wheelset rolling state, the signals of all three accelerometers (see Figure 2) were analyzed. Due to *Parseval's Relation*, the magnitude of the *eigenvalues* equals the mean signal power projected onto the *Characteristic Functions*. Figure 3 shows the three *eigenvalues* for each experiment. It can be observed, that there is a correlation between the yaw angles and the obtained *eigenvalues*. However, we are not interested in determining the yaw angle this way, but to measure the intensity of the wheelset dynamics. Obviously this does not increase linearly with the yaw angle. At small yaw angles (1.5 mrad), the *eigenvalues* are equal to those for *zero* yaw. This result coincides with observations during the experiments. Changes in *wheelset rolling state* could not be seen or heard. At larger yaw angles (2.5 mrad), vibrations at the wheel/rail-roller test-rig increased and at yaw angles of 3.5 mrad the vibrations increased drastically and an additional noise could be heard. This experiment produced metal powder on the floor. An obvious sign for the deterioration of the wheels.

Figure 4 show the projection of the *Characteristic Functions* onto the sensors 'X', 'Y' and 'Z' for each experiment. The *Characteristic Functions* have three components. Since the accelerometers are oriented along the three body-fixed wheelset-axes (Figure 2), the *Characteristic Functions* describe the principal directions of the wheelset vibration. The first *Characteristic Function* (black line) resembles the direction of wheelset vibration with the largest *kinetic energy*. Its projection shows, that this motion occurs mainly in z-direction, for any yaw angle. However, as the yaw angle increases, vibration in y-direction becomes more powerful. This can be observed by the increase of the y-component of the principal motion (first *Characteristic Function*).

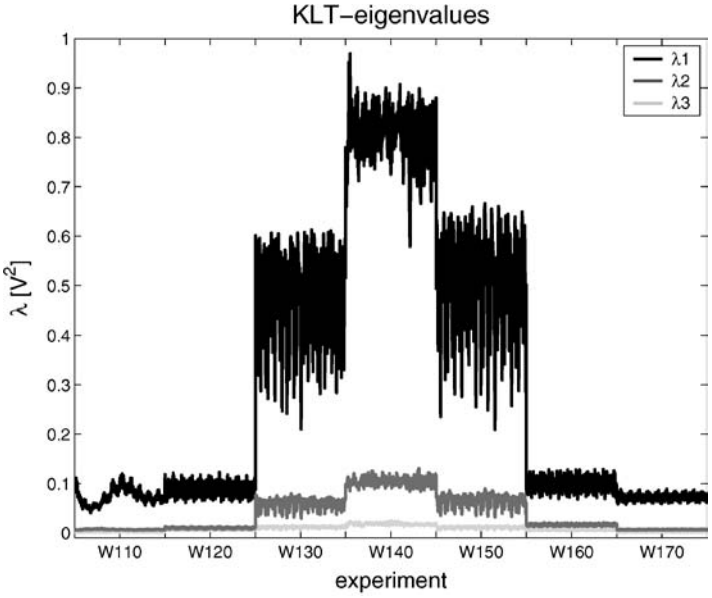

Figure 3. KLT-*surrogate power.*

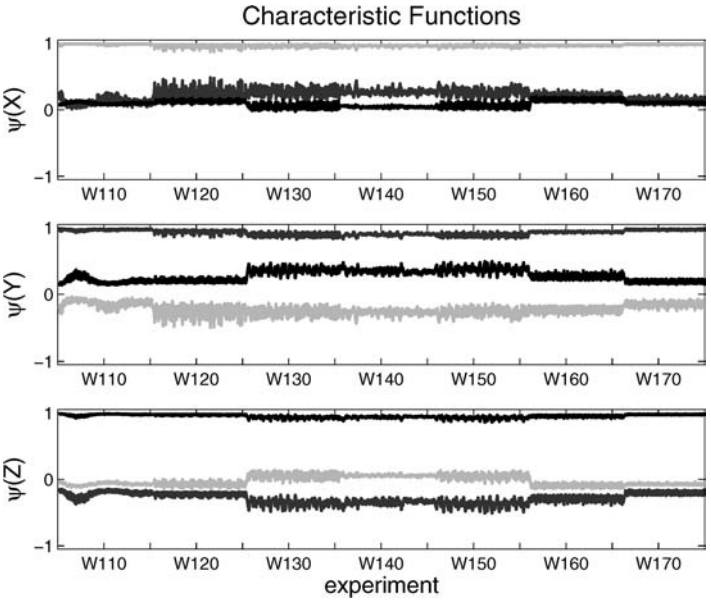

Figure 4. KLT *characteristic function.*

4.5. Application for Model Order Reduction

Although the discussion in Section 4 focuses on the state analysis of complex non-linear dynamical systems, there are two ways to apply this approach for model order reduction as well:

On the one hand, the system order can be reduced *before* modeling by KLT decomposition, if the system of interest physically exists and its dynamics are measurable. The state analysis by means of KLT

can be used to determine the surrogate eigenforms,[11] *Characteristic Functions* of the system, that can be defined as the new, 'effective DOF'. Then, the system can be modeled based on these new DOF. For this purpose, tests are performed and the dynamics of the system are measured. The KLT decomposes the dynamics into the surrogate eigenforms and the corresponding *Weighing Factors*. For modeling purposes, only those surrogate eigenforms that have a comparable large eigenvalue are considered. Thus, the number of DOF is limited forehand to the number of DOF that are necessary to capture a given fraction of the kinetic system energy.

Alternatively, the system order can also be reduced *within* the modeling process. Therefor, the PDEs are expanded in a truncated Galerkin-ansatz, as discussed in Section 3.2. In this case, the state analysis introduced in Section 4 can be regarded as an extension of previous approaches: The state analysis by means of KLT accounts for parameter changes of the investigated system. The model reduction technique discussed in Section 3.2 requires the system dynamics to be stationary. Parameter changes may qualitatively alter the system dynamics, thus leading to different surrogate eigenforms. The state analysis by means of KLT can be used to detect these changes and to distinguish between different '*states of system dynamics*' or different parameter settings, respectively. After the simulation of the complete set of PDEs with varying parameters, the model order can be reduced for each *state of system dynamics* individually, as discussed in Section 3.2.

5. Conclusion

A variety of applications for the KLT have been reported ranging from data compression to template matching and model order reduction. Some popular applications of the KLT have been discussed in this paper. In addition to the current list, we have introduced the KLT as a powerful tool to monitor the transient dynamics of railway wheelsets. The underlying investigation of Section 4 aims at characterizing the *rolling state* of railway wheelsets. For this purpose, the accelerations at a wheelset suspension are measured and analyzed by means of KLT. Mathematical proof is provided, showing that the *eigenvalues* emphasize changes in the *wheelset rolling state*. Analysis results show that the *Characteristic Functions* describe the principal directions of wheelset vibration. For the experimental set-up, the wheelset motion occurs mainly in vertical direction. Therefore, the *Characteristic Functions* do not display changes in the *wheelset rolling state* as distinct as the *eigenvalues*. However, if more sensors are applied and more accelerations are measured, the resolution of the surrogate eigenforms of the wheelset dynamics will improve. Thus, the *Characteristic Functions* will become more important for the characterization of the *wheelset rolling state*. Currently, the authors are investigating the benefit of an increase in the number of acceleration sensors.

Acknowledgements

The authors are grateful to Professor Meinke, Professor Popp, Dr Ullrich and Dipl.-Ing. Reicke for their fruitful cooperation in the project "Laufzustandsmonitoring von Eisenbahnfahrzeugen". We are thankful for financial support of this research to the Bundesministerium für Bildung und Forschung (BMBF), Germany, under the contract 13N-8093.

[11] See Section 4.3.2.

References

1. Mertins, A., *Signal Analysis*, Wiley, Chichester, UK, 1999.
2. Sirovich, L., 'Turbulence and the dynamics of coherent structures', *Quarterly Applied Mathematics* **45**(3), 1987, 561–582.
3. Lumley, J. L., 'The structure of inhomogeneous turbulent flows', in *Atmospheric Turbulence and Radio Wave Propagation*, A.M. Yaglom and V.I. Tatarsky, Nauka, Moskow, 1967, 166–178.
4. Dellnitz, M., Golubitsky, M., and Nicol, M., 'Symmetry of attractors and the Karhunen–Loève decomposition', in *Trends and Perspectives in Applied Mathematics*, Applied Mathematical Sciences 100, F. John, J. E. Marsden and L. Sirovich (eds.), Springer-Verlag, New York, 1994, pp. 73–108.
5. Holmes, P., Lumley, J. L., and Berkooz, G., *Turbulence, Coherent Structures, Dynamical Systems and Symmetries*, Cambridge Monographs on Mechanics, Cambridge University Press, Cambridge, 1996.
6. Newman, A. J., Model reduction via the Karhunen–Loève expansion part I: An exposition, University of Maryland, Technical Report, *T.R.96-32*, 1996.
7. Steindl, A., Troger, H., and Zemann, J. V., 'Nonlinear Galerkin methods applied in the dimension reduction of vibrating fluid conveying tubes', in *Proceedings of 4th International Symposium on Fluid–Structure Interactions, Aeroelasticity, Flow-Induced Vibration and Noise*, M. P. Paidoussis, A. K. Bajaj and T. C. Corke (eds.), AD-Vol. 53-1, ASME, 1997, pp. 131–156.
8. Kirby, M., 'Reconstruction of phase space from PDE simulations', *Zeitschrift für angewandte Mathematik und Physik (ZAMP)* **43**, 1992, 999–1022.
9. Newman, A. J., 'Model reduction via the Karhunen–Loève expansion part II: Some elementary examples, University of Maryland, Technical Report, *T.R.96-33*, 1996.
10. Kreuzer, E. and Kust, O., 'Mechanical modelling of drill-strings', *Archive of Applied Mechanics* **67**, 1996, 68–80.
11. Kreuzer, E. and Kust, O., 'Controlling torsional vibrations through proper orthogonal decomposition', in *Interaction Between Dynamics and Control in Advanced Mechanical Systems*, D. H. van Campen (ed.), Kluwer Academic Publishers, Dordrecht, The Netherlands, 1997, pp. 207–214.
12. Kreuzer, E. and Struck, H., 'Mechanical modelling of drill-strings', in *PAMM – Proceedings of Applied Mathematics and Mechanics*, Vol. 3-1, GAMM, 2003, pp. 88–91.
13. Kust, O., 'Selbsterregte Drehschwingungen in schlanken Torsionssträngen', Nichtlineare Dynamik und Regelung, Dissertation, VDI Verlag, Reihe 11, Schwingungstechnik, Düsseldorf, 1998.
14. Pentland, A., Picard, R. W., and Sclaroff, S., 'Photobook: Content-based manipulation of image databases, Massachusetts Institute of Technology', *Media Lab. Percept. Comput. Technical Report* **255**, 1993.
15. Uenohara, M. and Burton, T., 'Use of Fourier and Karhuhen–Loève decomposition for fast pattern matching with a large set', *Transaction on Pattern Analysis and Machine Intelligence* **19**(8), 1997, 891–898.
16. Sovakar, A., Scholl, I., and Neuschaefer-Rube, C., 'Verfolgung und Analyse von Stimmlippenkonturen in stroboskopischen Videosequenzen', in *Bildverarbeitung für die Medizin 1996*, T. M. Lehmann, I. Scholl, and K. M. Spitzer (eds.), Verlag der Augustinus Buchhandlung, Aachen, 1996, pp. 235–240.
17. Adam, D. R., 'Processing, feature extraction and classification of body surface potential maps', in *Advances in Processing and Pattern Analysis of Biological Signals*, I. Gath and G. F. Inbar (eds.), Plenum, New York, 1996, pp. 307–318.
18. Horowitz, F. G., Bone, D., and Veldkamp, P., 'Karhunen–Loève based iterated function system encodings', in *Proceedings PCS'96 of International Picture Coding Symposium*, Vol. 2, 1996, pp. 409–413.
19. Wickerhauser, M. V., *Adaptive Wavelet-Analysis, Theorie und Software*, Vieweg, Braunschweig, 1996.
20. Popp, K. (ed.), *Detection, Utilization and Avoidance of Nonlinear Dynamical Effects in Engineering Application*, Final Report of a Joint Research Project Sponsored by the German Federal Ministry of Education and Research, Shaker Verlag, Aachen, 2001.
21. Meinke, P., Meinke, S., and Blenkle, C., 'Nichtlinearitätssensor für den Laufzustand von Radsätzen', in *Detection, Utilization and Avoidance of Nonlinear Dynamical Effects in Engineering Application*, K. Popp (ed.), Final Report of a Joint Research Project Sponsored by the German Federal Ministry of Education and Research, Shaker Verlag, Aachen, 2001, pp. 131–156.
22. Popp, K. and Schiehlen, W. (eds.), *System Dynamics and Long-Term Behaviour of Railway Vehicles, Track and Subgrade*, Springer Verlag, Berlin, 2002.
23. Ertz, M., 'Temperatur, Materialbeanspruchung und Kraftschluss im Rad-Schiene-Kontakt', Dissertation, VDI Verlag, Reihe 12, Verkehrstechnik/Fahrzeugtechnik, Düsseldorf, 2003.
24. Kalker, J. J., 'On the Rolling Contact of Two Elastic Bodies in the Presence of Dry Friction', Dissertation, Delft University of Technology, 1967.
25. Küsel, M., 'Wellige Verschleissmuster auf Laufflächen von Eisenbahnrädern', Dissertation, Braunschweiger Schriften zur Mechanik, Technische Universität Braunschweig, 2002.

26. Troger, H. and Steindl, A., *Nonlinear Stability and Bifurcation Theory, An Introduction for Engineers and Applied Scientists*, Springer, Wien, 1991.
27. Aubry, N., Guyonnet, R., and R. Lima, 'Spatio-temporal analysis of complex signals: Theory and applications', *Journal of Statistical Physics* **64**(3/4), 1991, 683–739.
28. Sirovich, L., 'Chaotic dynamics of coherent structures', *Physica D* **37**, 1989, 126–143.